BASIC SCIENCE

Nanomedicine: Nanotechnology, Biology, and Medicine
24 (2020) 102106

Original Article

nanomedjournal.com

Zileuton™ loaded in polymer micelles effectively reduce breast cancer circulating tumor cells and intratumoral cancer stem cells

Petra Gener, PhD[a,*,1], Sara Montero[a,c,1], Helena Xandri-Monje[a], Zamira V. Díaz-Riascos, PhD[a,b], Diana Rafael, PhD[a,c], Fernanda Andrade, PhD[a,d,e], Francesc Martínez-Trucharte[a], Patricia González[a,c], Joaquin Seras-Franzoso, PhD[a], Albert Manzano[a], Diego Arango, PhD[f], Joan Sayós, PhD[c,g], Ibane Abasolo, PhD[a,b,c,*], Simo Schwartz JrMD, PhD[a,c,*]

[a]*Drug Delivery and Targeting Group, Molecular Biology and Biochemistry Research Centre for Nanomedicine (CIBBIM-Nanomedicine), Vall d'Hebron Institut de Recerca, Universitat Autònoma de Barcelona, Barcelona, Spain*

[b]*Functional Validation & Preclinical Research (FVPR), CIBBIM-Nanomedicine, Vall d'Hebron Institut de Recerca, Universitat Autònoma de Barcelona, Barcelona, Spain*

[c]*Networking Research Centre for Bioengineering, Biomaterials, and Nanomedicine (CIBER-BBN), Instituto de Salud Carlos III, Zaragoza, Spain*

[d]*i3S - Instituto de Investigação e Inovação em Saúde, Universidade do Porto, Porto, Portugal*

[e]*INEB - Instituto Nacional de Engenharia Biomédica, Universidade do Porto,Porto, Portugal*

[f]*Biomedical Research in Digestive Tract Tumors, CIBBIM-Nanomedicine, Vall d'Hebron Institut de Recerca, Universitat Autònoma de Barcelona, Barcelona, Spain*

[g]*Immune Regulation and Immunotherapy, CIBBIM-Nanomedicine, Vall d'Hebron Institut de Recerca, Universitat Autònoma de Barcelona, Barcelona, Spain*

Revised 28 August 2019

Abstract

Tumor recurrence, metastatic spread and progressive gain of chemo-resistance of advanced cancers are sustained by the presence of cancer stem cells (CSCs) within the tumor. Targeted therapies with the aim to eradicate these cells are thus highly regarded. However, often the use of new anti-cancer therapies is hampered by pharmacokinetic demands. Drug delivery through nanoparticles has great potential to increase efficacy and reduce toxicity and adverse effects. However, its production has to be based on intelligent design. Likewise, we developed polymeric nanoparticles loaded with Zileuton™, a potent inhibitor of cancer stem cells (CSCs), which was chosen based on high throughput screening. Its great potential for CSCs treatment was subsequently demonstrated in *in vitro* and in *in vivo* CSC fluorescent models. Encapsulated Zileuton™ reduces amount of CSCs within the tumor and effectively blocks the circulating tumor cells (CTCs) in the blood stream and metastatic spread.

Key words: Cancer stem cells (CSC); Circulating tumor tells (CTC); Nanomedicine; Polymeric micelles; Zileuton™

Despite the latest progress in early diagnosis and more effective treatments, advanced breast cancer is still an incurable disease.[1,2] Particularly aggressive is the Triple Negative Breast Cancer (TNBC), which does not respond to current hormonal therapy and medicines targeting HER2 receptors, because of the absence of estrogen–, progesterone –, and Her2– surface receptors in tumor cells. It has been suggested that tumor progression and dissemination are mediated by the presence of specific Cancer Stem Cells (CSCs) subpopulations within the tumor. CSCs are also thought to be responsible for cancer relapse and of being intrinsically resistant to most current treatments. Accordingly, CSCs are thus responsible for many therapeutic failures.[3–5] Unfortunately, there are no effective treatments yet targeting CSCs and their metastatic spread to distal organs.

Statement of funding

The authors declare no potential conflicts of interest

*Corresponding authors at: Drug Delivery and Targeting Group, Molecular Biology and Biochemistry Research Centre for Nanomedicine (CIBBIM-Nanomedicine), Vall d'Hebron Institut de Recerca, Universitat Autònoma de Barcelona, Barcelona, Spain.

E-mail addresses: petra.gener@vhir.org (P. Gener), ibane.abasolo@vhir.org (I. Abasolo), simo.schwartz@vhir.org (S. Schwartz).

[1] These authors contributed equally.

https://doi.org/10.1016/j.nano.2019.102106

Therefore, in order to increase patient survival, it has become essential to develop new therapeutic strategies against CSC to successfully eradicate advanced cancer and prevent metastasis.

Unfortunately, many prospective drugs do not have sufficient solubility or adequate pharmacokinetics to reach good efficacy and toxicity profiles for clinical use. In this context, specific nano-sized drug delivery systems (nano-DDS) offer the possibility of converting agents with low therapeutic profile into forthcoming clinical drug candidates. Further, nano-encapsulation facilitates the administration of hydrophobic agents while protecting them during circulation, lowering the undesired side effects associated with a systemic, non-controlled distribution of the drug. Nanomedicines can also evade Multi Drug Resistant mechanisms (*i.e.*, MDR channels) and increase drug's intracellular accumulation, improving the efficacy of the treatment.[4,6,7]

We have used two recently characterized fluorescent breast CSC models to identify by high throughput screening potential therapeutic target candidates in CSCs.[8,9] These models express tdTomato (red fluorescence) under the control of the CSC specific promoter, ALDH1A1. Thus, tdTomato fluorescence is detected exclusively in the CSC subpopulation, while differentiated cancer cells (non-CSCs) do not express the fluorescent marker. This system allows not only to segregate CSCs from non-CSCs subpopulations, but also to monitor the biological performance of CSCs *in situ;* before, during and after treatment.[8–11] Our data revealed arachidonate 5-lipoxygenase (5-LO) gene (Alox5) as a potential therapeutic candidate in breast CSCs. Recently, ALOX5 was also identified as a critical regulator of CSCs from Chronic Myeloid Leukemia (CML).[12] Moreover, we have recently demonstrated that siRNA inhibition of Alox5 is able to downregulate the expression of the gene *in vitro* and also of decreasing invasion and malignant transformation of breast CSCs.[13]

Zileuton™ is a specific marketed drug inhibitor of ALOX5, approved by the FDA as an anti-leukotriene oral drug for the treatment of asthma.[14,15] Its potential use as anticancer drug has been recently addressed in clinical trials. Thus, no safety issues related to oral administration of Zileuton™ were reported in a clinical trial (Safety; phase 1) in combination with Dasatinib (Sprycel®) (NCT02047149) and with Imatinib Mesylate (Gleevec) (NCT01130688) respectively, in patients with CML. Unfortunately, additional randomized phase-II trails to study the efficacy of oral Zileuton™ in cancer patients in combination with *Standard-of-Care* treatments have not yield positive results, so far (Clinical.Trials.gov). Most likely, the need of an intravenous administration, the high hydrophobicity of the drug and its high IC_{50}, hamper its potential clinical use in the oncology field. Here, we report on the anticancer and anti-metastatic effects of new Zileuton™ -loaded polymeric micelles, using *in vivo* breast CSCs models. Our data show significant intratumoral reduction of CSCs *in vivo*, and also a strong reduction of circulating cancer cells and CSCs in the blood in these models.

Methods

Microarray performance and validation

In total 8 RNA samples, comparing 2 technical replicates of tdTomato positive ($tdTomato^+$) and tdTomato negative ($tdTomato^-$) samples (corresponding to CSC and non-CSC) sorted from two different cell lines (MCF7-ALDH1A1:tdTomato, MDA-MB-231-ALDH1A1:tdTomato) (details in supplementary data) were analyzed by microarray. For this, 100 ng of total RNA was labeled using LowInputQuick Amp Labeling kit v6.5 (Agilent 5190-2305) following manufacturer instructions. The labeled cRNA was hybridized to the Agilent SurePrint G3 Human gene expression 8×60K microarray (ID039494) according to the manufacturer's protocol. The arrays were scanned on an Agilent G2565CA microarray scanner at 100% PMT and 3 μm resolution. Raw data were taken from the Feature Extraction output files and were corrected for background noise using the normexp method.[16] To assure comparability across samples we used quantile normalization.[17] Differential expression analysis was carried out in noncontrol probes with an empirical Bayes approach on linear models (limma), applying a paired test.[18] Results were corrected for multiple testing according to the False Discovery Rate (FDR) method.[19] Obtained results were confirmed by qPCR and flow cytometry (details in supplementary data). Clinical and expression data of *ALOX5* were obtained from The Cancer Genome Atlas (TCGA) for breast invasive cancer collection, in order to correlate these two features. Also, expression microarray data from the same portal were used to evaluate *ALOX5* overexpression with ovarian serous cystadenocarcinoma, lung adenocarcinoma and colon adenocarcinoma.

In vitro functional validation of free and encapsulated Zileuton™

To validate efficacy of Zileuton™ *in vitro,* we performed i.) Cell viability assay ii.) CSC resistance assay, and iii.) Cell Transformation Assay (Anchorage-Independent Growth Assay) (experimental details are in supplementary data).

Production and physicochemical characterization of PMs for Zileuton™ delivery

PMs were prepared using the thin-film hydration technique and characterized them by Dynamic Light Scattering (DLS) (Malvern Instruments), Transmission Electron Microscopy (TEM) and Cryo-Transmission Electron Microscopy (Cryo-TEM) (details in supplementary data).

Furthermore; i.) Entrapment efficiency ii.) PMs stability, and iii.) PMs internalization were evaluated (details in supplementary data).

In vivo preclinical validation of PM-Zileuton™

Animal care was handled in accordance with the Guide for the Care and Use of Laboratory Animals of the Vall d'Hebron University Hospital Animal Facility, and the Animal Experimentation Ethical Committee at the institution approved the experimental procedures. All the *in vivo* studies were performed by the ICTS "NANBIOSIS" of CIBER-BBN's *In Vivo*

Experimental Platform of the Functional Validation & Preclinical Research (FVPR) area (CIBBIM-Nanomedicine, Barcelona, Spain).

Orthotopic breast cancer models

MCF-7 and MDA-MB-231 breast cancer cells were orthotopically inoculated into mammary fat pad (i.m.f.p) as previously described.[8,9,20,21] In detail, MDA-MB-231 cells and MCF-7 cells suspended with Matrigel (1:1) (BD Bioscience, Bedford, MA, USA) were respectively implanted into the right abdominal mammary fat pad (i.m.f.p.) of NOD-SCID mice (Supplementary data). MCF-7 tumor bearing mice were also subcutaneously injected with estrogen pellets (17β-Estradiol, 0.36 mg/pellet, 90 days release; Innovative Research of America, Sarasota FL, USA). Further, 3 days before i.m.f.p. inoculation their drinking water was supplemented with Baytril (Enrofloxacin) 0.08 mg/mL as a preventive measure to minimize the side effects from estradiol. Tumor growth was monitored twice a week by conventional caliper measurements ($D \times d2/2$, where D is the major diameter and d the minor diameter).

Toxicity

Female athymic mice were treated intravenously (i.v.) with 1.5, 5 and 15 mg/kg (n = 5/dose) 3 times per week during 3 weeks. Body weight changes and animal welfare were monitored along the assay. Animals were euthanized 1 h after the last administration and blood and tissue samples collected after gross necropsy.

Biodistribution

Ten mice were administered with a unique dose of PMs labeled with fluorescent dye DIR at 0.8 mg DiR/kg by i.v. administration route. Eight of these mice had i.m.f.p. MDA-MB-231 tumors and 2 mice without tumor were also included in the assay as a control to set the autofluorescence of the tissue. At 24, 44 and 72 h administration, tumor-accumulation and whole-body biodistribution were measured non-invasively by DiR fluorescence imaging (FLI) from the ventral and dorsal mouse views, using the IVIS Spectrum (Perkin Elmer) imaging system analyzed using Living Image® 4.5.2 software (PerkinElmer). In addition, at 72 h post administration end time point, plasma, tissue and tumor samples were collected, weighed and processed for *ex vivo* imaging. The fluorescence signal in *ex vivo* images was quantified in Radiant Efficiency units and referred to the tissue weight following procedures previously described.[8,20,21]

Efficacy

In order to test the effects of PM-Zileuton™ in the tumor growth and in the CSC population, orthotopic breast cancer models were generated using freshly sorted tdTomato+ cells (0.6×10^6 cells / mouse for the MCF-7 cell line and 0.1×10^6 cells/animal for the MDA-MB-231 cell line). Animals were then treated with i.v. administration of PM-Zileuton™ (15 mg/kg), 3 times per week during 3 weeks. One day (MDA-MB-231) or 7 days (MCF-7) after the last administration animals were euthanized and blood and tumor samples were collected for the analysis of CSC content. To measure the extent of lung metastasis *ex vivo* bioluminescent imaging (BLI) was also performed using the IVIS Spectrum after administering 150 mg/kg of luciferin to mice. Immediately after necropsy, lung tissues were placed individually into separate wells containing 300 μg/mL of D-luciferin, and imaged and quantified using Living Image® 4.5.2 software.[21] Determination of circulating tumor cells in the blood stream and the content of tdTomato+ cells within the tumor was performed by flow cytometry (details in supplementary data). For this all injected cells expressed GFP under CMV promotor. We analyzed all alive cells ($Dapi^-$) that emitted green fluorescence and quantified the ones which were also $tdTomato^+$ as CSC.

Results:

ALOX5 is a breast CSC specific therapeutic target candidate

In order to design an effective anti-cancer therapy, we analyzed transcriptome of CSCs sorted from two different CSC fluorescent models; MDA-MB-231-ALDH1A1:tdTomato, a basal-like breast cancer cell line highly aggressive and chemo-resistant, and MCF7-ALDH1A1:tdTomato, a luminal breast cancer cell line. Correlation-based clustering analysis of microarray data revealed substantial disparity due to epithelial (MCF7) and mesenchymal (MDA-MB-231) characteristics of respective cell lines (Figure S1). Several mesenchymal markers (*e.g. VIM*, *CD44*, *SERPINE1/2*, *ESAM*) were clearly over-expressed in MDA-MB-231 cells and under-expressed in MCF7 cells. Contrarily, epithelial markers (*e.g. CD24*, *KRT6B*, *KRT8*, *KRT18*, *CDH1*) were over-expressed in MCF7 cells and under-represented in MDA-MB-231 cells[25] (Figure S1). These pronounced differences between cell line characteristics, partly concealed the expected differences in reported CSC markers (*e.g. KLF5*, *DUSP6*, *ITGB2*, *ALDH1A1*, *SOX9/2*, *NOTCH2/4*, *MUC16*, *GRHL2*) comparing CSCs with non-CSCs[1] (Figure S1). Nonetheless, we identified 75 up-regulated genes (FC > 2) and 58 down-regulated genes (FC < 0.5) in CSCs segregated from both, MCF7 and MDA MB 231 cell lines. Several candidates were chosen for further confirmation based on the uniformity of these increased levels found in CSCs in all related samples and/or their relationship with CSC biology (Figure 1, *A*).

In MDA-MB-231 CSCs, we confirmed increased mRNA expression of; *ALOX5* (Arachidonate 5-Lipoxygenase), *CMKLR1* (Chemokine like receptor 1), *BST2* (Bone Marrow Stromal Cell Antigen 2), *SNAI1* (Snail family zinc finger 1). In MCF7 CSCs, we confirmed increased expression of; *TGFB2* (Transforming Growth Factor β 2), *ALOX5*, *SPARC* (Secreted Protein, Acidic, Cysteine-Rich), *PTPRE* (Protein Tyrosine Phosphatase, Receptor type, E), *EGR4* (Early Growth Response 4), and *SNAI1/2*. Contrary to the microarray analysis, validation through q-PCR did not prove any significant difference between CSC and nonCSC regarding BST2 and *LIPA* in MCF7, and *EGR4*, *PTPRE*, *LIPA*, *TGFB2* and *SNAIL2* genes in MDA-MB-231 (Figure 1, *B*).

Only *ALOX5* was significantly overexpressed in both, MDA-MB-231 and MCF7 CSCs. Moreover, *in silico* analysis of data from 590 patients with invasive breast cancer, revealed over-expression of *ALOX5* mRNA (FC > 2) in 83.6% of total cases (Figure 1, *C*). However, no significant correlation with known

A

log2ratio_MCF7_CSC vz. MCF7_nonCSC	log2ratio_MDA231_CSC vz. MDA231_nonCSC	log2ratio_CSC vz. nonCSC	GeneName	FC_MCF7_CSC vz. MCF7_nnCSC	FC_MDA231_CSC vz. MDA231_nonCSC	FC_CSC vz. nonCSC	P.Value_CSC vz. nonCSC	Confirmed overexpression in MCF7 CSC	Confirmed overexpression in MDA231 CSC
			PGC	3.76	3.62	3.69	0.01	-	-
			ALOX5	5.15	2.50	3.59	0.00	yes	yes
			EGR4	3.33	2.80	3.05	0.04	no	no
			BST2	2.60	2.62	2.61	0.00	no	yes
			TGFB2	3.38	1.49	2.25	0.02	yes	no
			HLA-DRB5	2.34	2.15	2.24	0.01	-	-
			PTPRE	2.08	2.02	2.05	0.00	yes	no
			SNAI2	1.63	2.57	2.05	0.02	yes	no
			IL10RA	1.23	3.21	1.99	0.10	-	-
			GRM5	1.52	1.96	1.73	0.04	-	-
			LIPA	1.27	1.22	1.24	0.06	no	no
			TLR2	1.55	-1.09	1.19	0.45	-	-
			CMKLR1	-1.02	1.28	1.12	0.36	no	yes
			GATA4	1.04	1.17	1.11	0.29	no	-
			SNAI1	-1.02	-1.11	-1.06	0.59	yes	yes
			SPARC	-1.03	-1.28	-1.15	0.39	yes	no

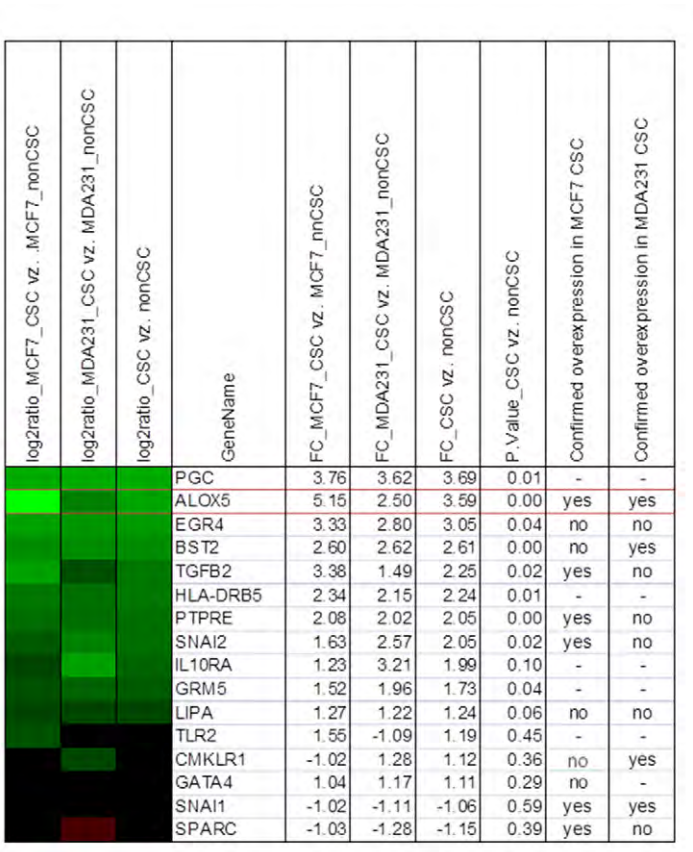

C

% Patients with FC [ALOX5] > 2	*Brest Cancer*	*Ovarian Cancer*	*Lung Cancer*	*Colorectal Cancer*
ALOX 5	***83.6***	***80.5***	***75***	***50.3***

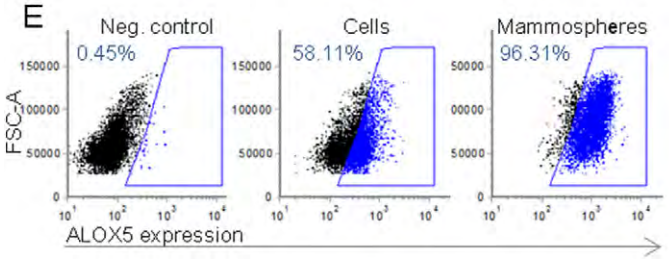

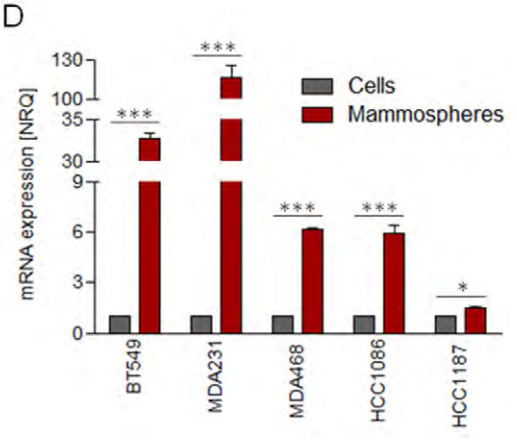

Figure 1. High-throughput microarray data from breast cancer cell lines.(**A**) Expression microarray analysis showing selected candidates for further validation by qPCR. FC = fold-change. *P* value >0.05 shown in light red, *P* value <0.05 shown in light green. (**B**) Relative expression levels of selected candidates in CSC in MCF-7 and MDA-MB-231 cell lines. Significant results with *P* value >0.05 are marked with *. Alox5 gene is upregulated in both cell lines. (**C**) ALOX5 expression levels for Breast Cancer, Ovarian Cancer, Lung Cancer and Colorectal Cancer according to *The Cancer Genome Atlas* (TCGA).(**D**) Alox5 expression in CSCs in breast cancer cell lines. In order to obtain a CSCs enriched population, cells were grown as mammospheres in low attachment conditions without FBS. (**E**) Increased expression of ALOX5 protein level was confirmed in MDA-MB-231 mammospheres. Significant results with *P* value ≤0.001 are marked with ***.

clinical pathological features of the patients was found (data not shown). Interestingly, clinical data also revealed over-expression of *ALOX5* mRNA in 80% of patients with ovarian cancer, 75% of patients with lung cancer and in 50% of patients with colorectal cancer. Increased *ALOX5* mRNA expression was further confirmed in a battery of triple negative breast cancer cell lines (TNBC), BT549, MDA-MB-231, MDA-MB-468, HCC1086, HCC1187, comparing normal cell culture conditions

(growing in attachment and with complete medium) with CSC culture conditions (growing in non-attachment and in serum depleted medium as mammospheres) (Figure 1, *D*). Moreover, the increase of ALOX5 protein level was confirmed in MDA-MB-231 CSC culture (Figure 1, *E*). Therefore, we have further explored ALOX5 prospects as therapeutic target candidate to develop anti-CSCs therapy.[13]

Significant antitumoral efficacy of Zileuton™ against CSCs mammospheres

To validate the antitumoral effects against CSCs of inhibiting ALOX5 we investigated the efficacy of a selective, FDA approved ALOX5 inhibitor; Zileuton™. First, we determined the half inhibitory concentration (IC_{50}) of Zileuton™ in MDA-MB-231 and MCF7 breast cancer cell lines. As expected, Zileuton™ was more effective against MCF7 than in more resistant and aggressive MDA-MB-231 cell line. Of note IC_{50} [MCF7] = 292 μM, IC_{50} [MDA-MB-231] = 461 μM (Figure S2). After, we determined the IC_{50} of Zileuton™ using pure tdTomato$^+$ CSCs subpopulation sorted from both cell lines. The IC50 was determined in two different cell culture conditions. On the one hand, in attachment conditions as normal cell culture conditions and on the other, in low attachment conditions as optimal conditions for CSCs culture. Interestingly, we observed increased efficacy of Zileuton™ in CSCs from both cell lines when CSCs were cultured in low attachment conditions; (IC_{50} [MCF7] = 29.4 μM, IC_{50} [MDA-MB-231] = 619 μM) compared to normal attachment culture (IC_{50} [MCF7] = 499 μM, IC_{50} [MDA-MB-231] = 852 μM) (Figure 2, *A*). Of note, we could also determine that *ALOX5* expression is increased when CSCs are cultured as mammospheres (Figure 1, *D*, *E*).

Furthermore, Zileuton™ efficiently inhibited cellular growth in soft agar (transformation assay), which is a hallmark of CSCs, in a concentration dependent manner (Figure 2, *B*). Moreover, in order to compare the effect of Zileuton™, with Paclitaxel (PTX) and Abraxane™ (ABX), both drugs currently used in the clinics,[22,23] we evaluated the relative abundance of CSCs before and after treatment, respectively. However, in order to mimic chemotherapeutic cycles in a similar way than used as standard-of-care, CSC *in vitro* models were treated with Zileuton™, PTX and ABX for 72 h, and then cells left to recover in medium without drugs during 48 additional hours. Even though in all cases similar efficacy was reached, the relative abundance of tdTomato$^+$ CSCs increased significantly after PTX and ABX treatment while remarkably, this was not observed after Zileuton™ treatment, particularly in the resistant line, MDA-MB-231 (Figure 2, *C*).

Production and physico-chemical characterization of pluronic-F127 polymeric micelles loaded with Zileuton™

Zileuton™ is a highly hydrophobic compound that cannot be administrated i.v. to reach the required therapeutic effect. Because of this, we encapsulated Zileuton™ in the inner core of polymeric micelles formed by amphiphilic polymer Pluronic® F127, by thin-film hydration technique.[24–26] The micelles obtained (PM-Zileuton™) showed a mean diameter of 25 nm, with a low polydispersity index (≤ 0.2) (Figure 3, *A*). These data were confirmed by TEM and Cryo-TEM images, where it was possible to observe micelles of small size in the region of 25 nm with spherical morphology (Figure 3, *B*). DLS measurements performed one and two months after the preparation of the polymeric micelles confirmed their high stability at room temperature, since their physico-chemical features did not change over time (Figure S3, *A*). In addition, we tested the stability of PM-Zileuton™ in bovine serum. Accordingly, no aggregates appeared during 24 h in medium with FBS (50%) (Figure S3, *B*). Further, we could also establish 0.075 μM Zileuton™ stock as maximal encapsulatable dose, with up to 96% of encapsulation efficacy. These results were confirmed by UPLC. Of note, it was impossible to further increase the concentration of encapsulated Zileuton™, because at higher concentration Zileuton™ precipitated and formed crystals during the rehydration step.

Moreover, with the perspective to allow future clinical studies, we also demonstrated stability and efficacy of lyophilized PM-Zileuton™. Accordingly, no significant differences regarding size and *in vitro* efficacy were observed after the lyophilization and rehydration processes (Figure 3, *C*).

Finally, internalization studies were also performed. Fluorescently tagged PMs were internalized as early as one minute after its addition to cell culture in both cell lines (results of MCF7 cell line not shown). After 10 min all cells have internalized the tagged micelles and the intracellular amount of them followed to increase afterwards, as it was perceived by a constant increase of the fluorescence intensity (Figure 4, *A*). Interestingly, no significant differences regarding PMs internalization were observed between the subpopulations of CSCs and non-CSCs, respectively (Figure 4, *A*). By confocal microscopy, we observed lysosomal co-location of PMs tagged with 5-DTAF after 1 h and also 24 h after internalization (Figure 4, *B*).

Strong inhibition of CSCs by PM-Zileuton™ in in vitro and in vivo breast CSC models

Once polymeric micelles were produced and characterized, its functional validation was assessed. First, a biodistribution study was performed with DiR labeled PM™ in tumor bearing mice. *In vivo* fluorescent imaging (FLI) clearly showed that micelles tend to accumulate in the tumor area (mammary gland in the left caudal area). Fluorescent signal was also observed in the abdominal area, corresponding to the liver. *Ex vivo* imaging and quantification of the fluorescent signal were performed 24 and 72 h post-injection showing the kinetics of the micelles biodistribution and excretion (Figure 5). Data revealed that micelles were being accumulated in the tumor with a relative accumulation of 9.11% +/− 2.68% of total FLI signal per gram of tissue at 24 h that was kept practically invariable at 72 h post-administration (8.21% +/− 0.83% FLI/g). Liver and spleen also retained the micelles in levels comparable to those in the tumor. On the other hand, fluorescent signals in plasma, kidneys, lungs and muscle showed clearly descended between 24 and 72 h, indicating that micelles were cleared out by these organs.

Second, *in vitro* and *in vivo* efficacy was tested. Accordingly, the IC_{50} of Zileuton™ was significantly decreased after its encapsulation into PMs (IC_{50} [PM-Zileuton™] = 304 μM). Of

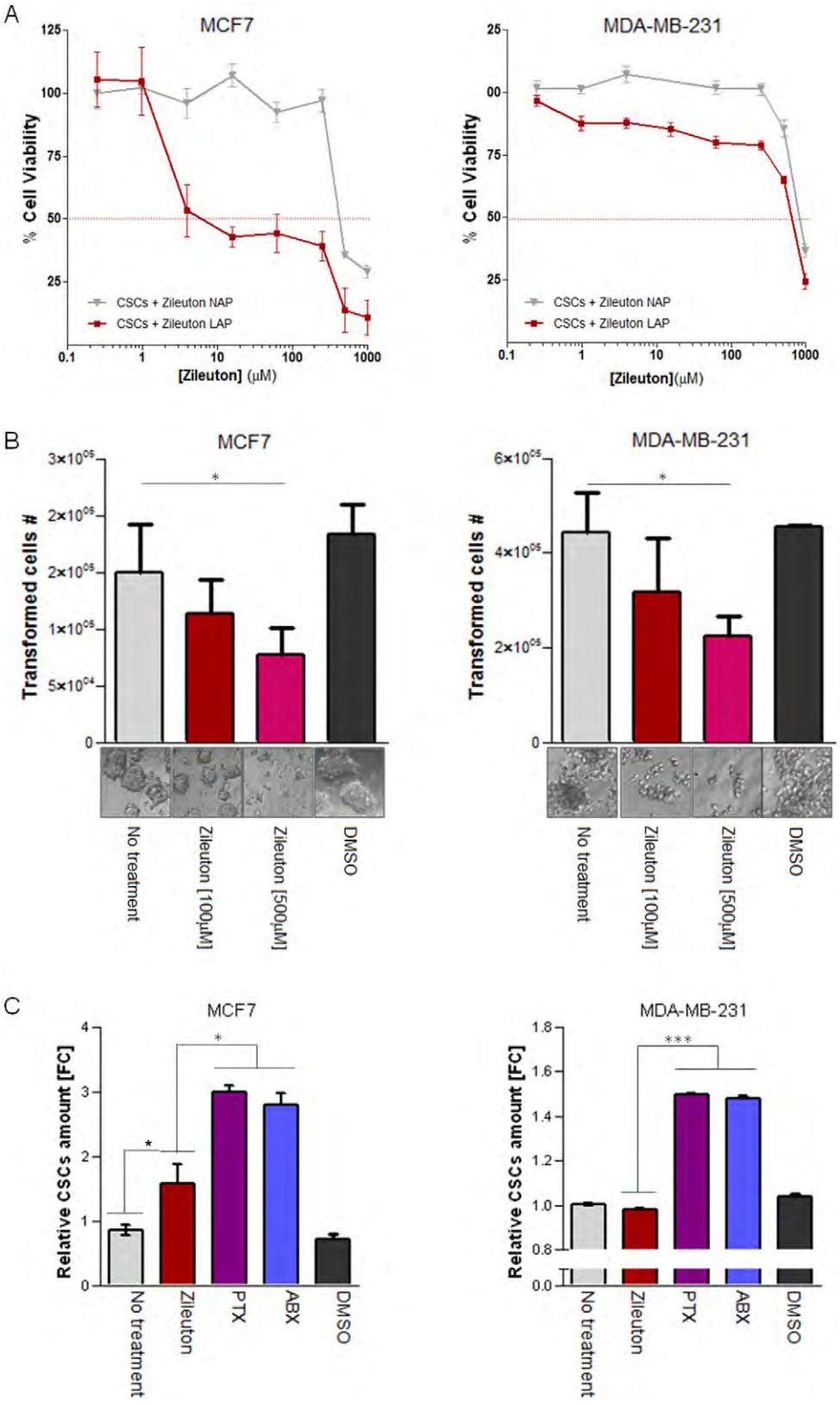

Figure 2. *In vitro* cell viability and transformation capacity of breast cancer cell lines and CSCs treated with Zileuton™.(**A**) Cell viability (MTT) assay for MCF7 and MDA-MB-231 CSCs treated with Zileuton™. Cells were grown in normal condition (NAP: normal attachment plates) and as mammospheres (LAP: low attachment plates). IC_{50} corresponds to the half maximal inhibitory concentration and is indicated by a discontinuous red line. Cells without treatment represent 100% of viability. (**B**) Transformation capacity (anchorage independent growth) of MCF-7 and MDA-MB-231 CSCs treated with Zileuton™. (**C**) Content of CSCs (tdTomato+) after treatment with Zileuton™ and ABX / PTX was quantified by flow cytometry in MCF-7 and MDA-MB-231 cell lines.

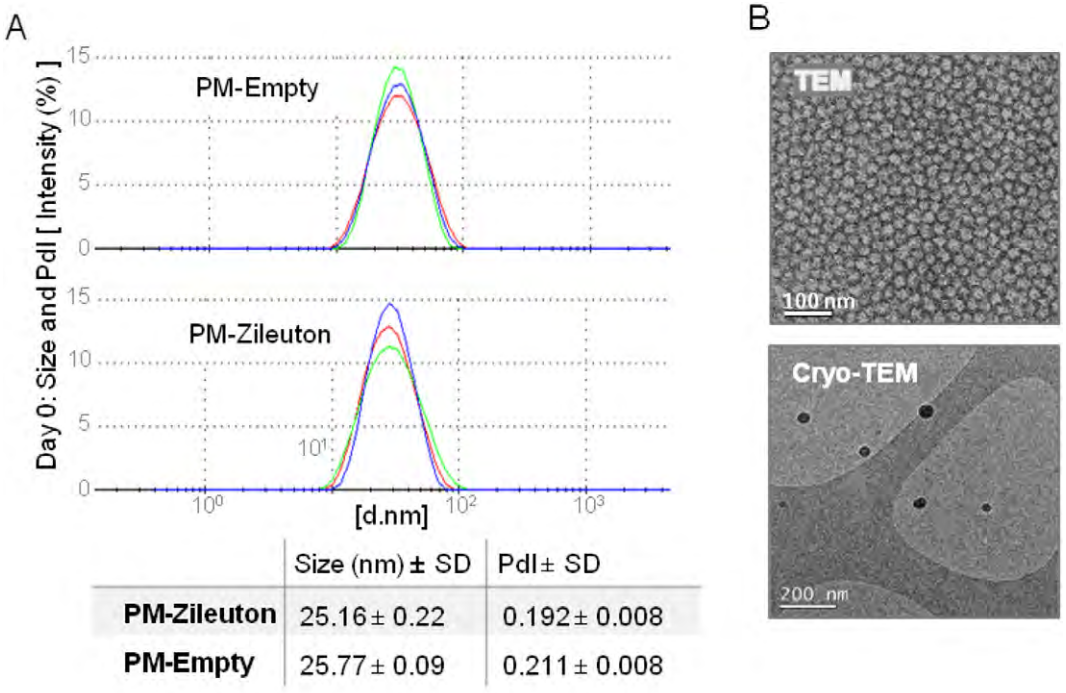

	Size (nm) ± SD	PdI ± SD
PM-Zileuton	25.16 ± 0.22	0.192 ± 0.008
PM-Empty	25.77 ± 0.09	0.211 ± 0.008

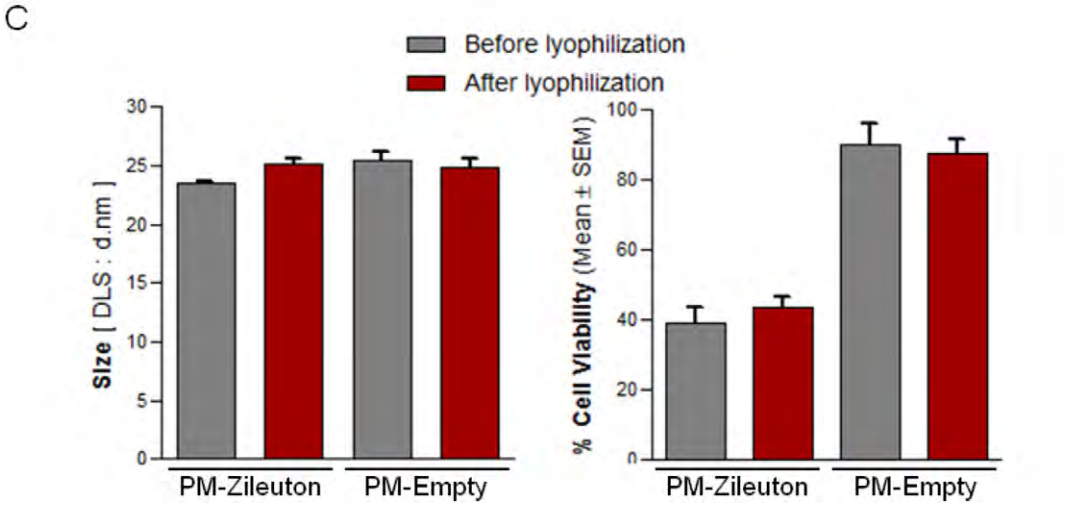

Figure 3. Physico-chemical characterization and cell internalization of PM-Zileuton™.(**A**) DLS size distributions by intensity with Z-average and PdI values of Polymeric micelles loaded with Zileuton™, and unloaded nanoconjugates. (**B**) Electron microscopy images; TEM technique / Cryo-TEM of polymeric micelles loaded with Zileuton™. (**C**) Mean diameters (nm) of PM-Zileuton™ and unloaded micelles, measured by DLS before and after lyophilization and MDA-MB-231 CSCs viability, measured before and after lyophilization.

note, unloaded polymeric micelles did not show any substantial toxicity (Figure 6, *A*). Further, the transformation capacity of the cells was significantly decreased by PM-Zileuton™ when compared to free Zileuton™ (Figure 6, *B*). Moreover, because CSCs growing as tumorspheres in low attachment are highly resistant to common treatment (PTX, ABX), we wondered if PM-Zileuton™ would be effective in these conditions. Remarkably, PM-Zileuton™ were able to reduce the viability of CSCs in low attachment conditions, while no effect was seen for PTX and ABX in these conditions (Figure 6, *C*). Moreover, we have compared the viability of CSCs in normal growth condition or in low attachment (mammospheres) after Zileuton™ treatment in combination with Abraxane or Paclitaxel. Even though no synergistic or additive effect was observed in combinatory treatment, Zileuton™ PMs significantly compromised the viability of MDA-MB-231 CSCs in all tested conditions (Figure S4).

Next, to determine possible *in vivo* adverse side effects, maximal feasible dose (MFD = 15 mg/kg) of PM-Zileuton™ was intravenously (i.v.) administrated into athymic mice. We did not observe significant loss of weight of the animals or any alterations in their overall well-being. Also, no macroscopic

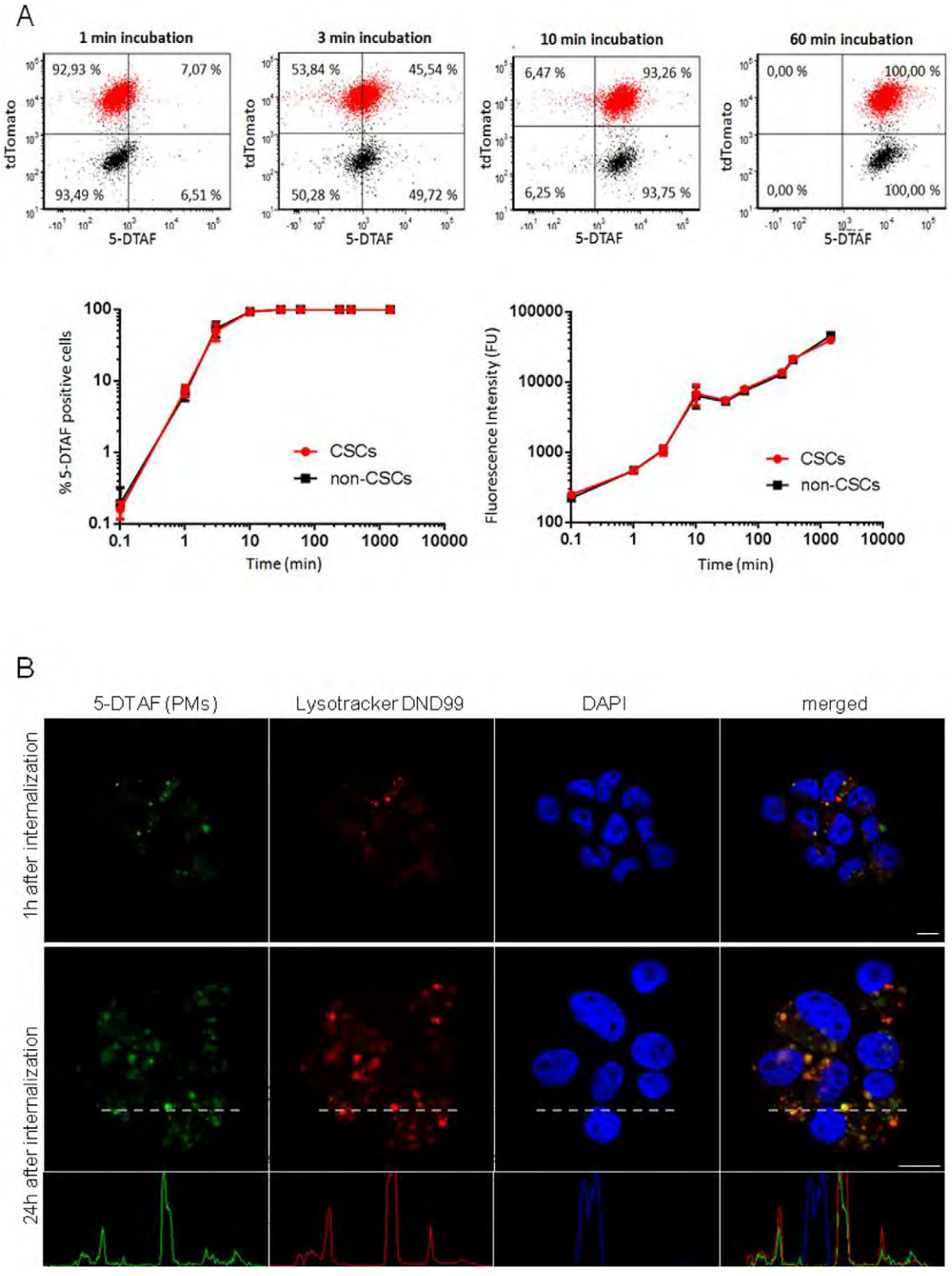

Figure 4. Internalization of PM-Zileuton™ in breast cancer cells.(**A**) Over time course quantification of CSCs (tdTomato+; red) and non-CSCs (tdTomato−; black) cellular uptake of fluorescently tagged PMs (PM-DTAF), reported as percentage of DTAF positive cells and relative increase of fluorescence intensity over time. For each sample, at least 10,000 individual cells were collected and the mean fluorescence intensity was evaluated. (**B**) The internalization of PM-Zileuton™ in breast MDA-MB-231 cancer cells was also observed by confocal microscopy 1 h and 24 h after internalization. Micelles were labeled with 5-DTAF (green fluorescence), lysosomes were labeled with Lysotracker DND99 (in red) and DAPI was used to visualize nuclei (in blue). The co-location of micelles and lysosomes was confirmed by fluorescence intensity plots over the illustrated dot line (24 h).

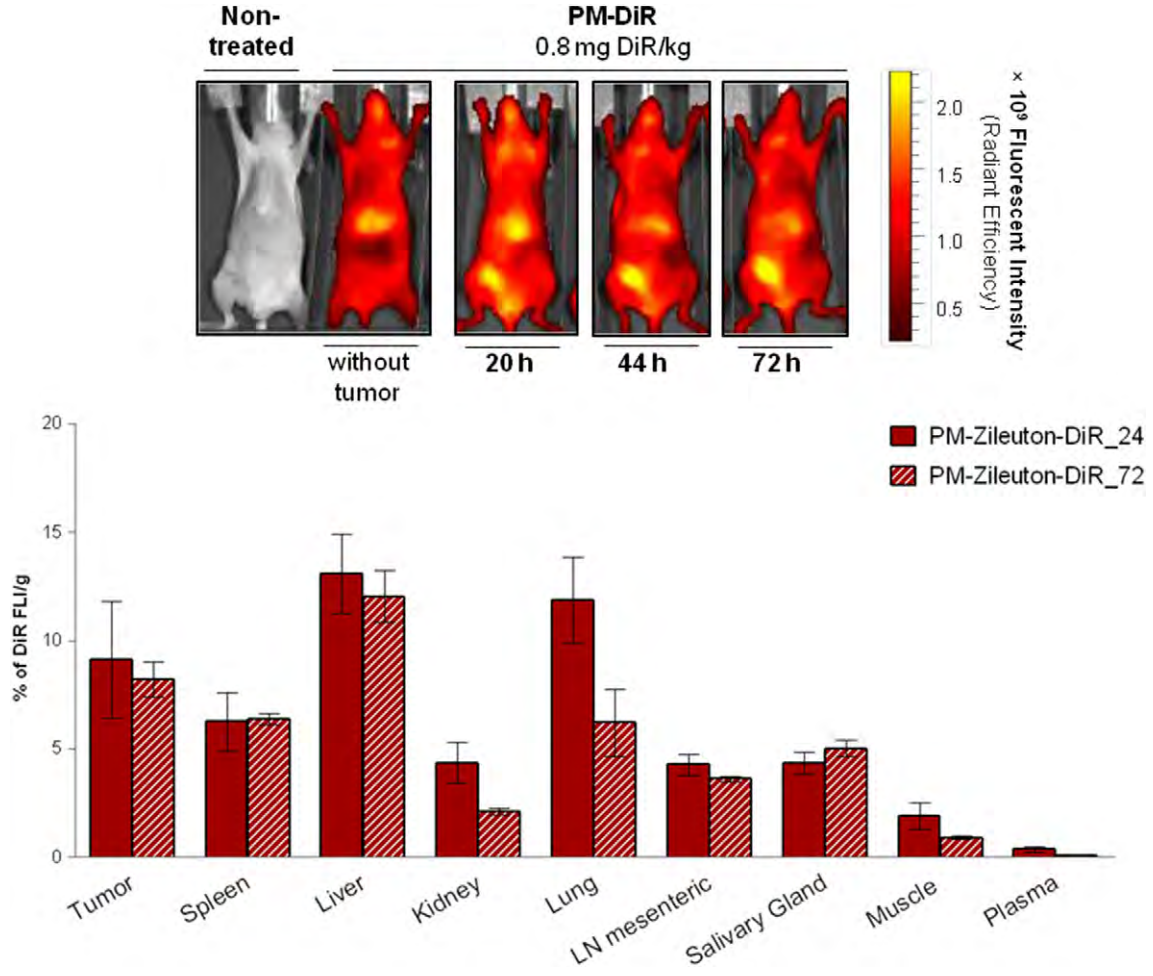

Figure 5. *In vivo* biodistribution of PM in mice with breast cancer orthotopic tumors. *In vivo* and *ex vivo* BLI of intravenously administered DiR labeled PM™ in athymic mice revealed that PM tended to accumulate in tumor tissues, being the clearance rate of nanoparticles in tumor lower than for other tissues. Fluorescent signal was observed the tumor and in the abdominal area, corresponding to the liver. *Ex vivo* imaging and quantification of the fluorescent signal were performed 24 and 72 h post-injection showing the kinetics of the micelles biodistribution and excretion.

alterations were found by gross necropsy and further histological evaluation (Figure S5).

Finally, we performed *in vivo* efficacy studies using orthotopic breast cancer models. For this, CSCs sorted from the MCF7 luminal breast cancer cell line and from the highly aggressive MDA-MB-231 basal-like breast cancer cell line were used. Cells were injected into mammary fat pad to ensure high CSCs content in the growing tumors. Remarkably though, PM-Zileuton™ significantly reduced almost by two-fold the content of CSCc in the treated tumors compared to non-treated animals, in both orthotopic models (Figure 7, *A*). CSCs decrease from 58% +/– 9% in vehicle-treated MDA-MB-231 tumors to 37.2% +/– 4.7% in PM-Zileuton™ treated ones, and from 33.43% +/– 3.18% to 17.98% +/– 6.25% in MCF-7 models, respectively. CSCs reduction was convoyed with the eradication of circulating tumor cells (CTC) after PM-Zileuton™ treatment in a metastatic MDA-MB-231 *in vivo* model (Figure 7, *B*). No CTC was detected in MCF7 *in vivo* model in any case (data not shown). As expected, reduction of CTC in MDA-MB-231 model was accompanied by a significant reduction of metastasis detected by BLI (Figure 7, *C*). In contrast, we have not observed differences in tumor growth comparing group of animals treated with vehicle or PM-Zileuton™ (Figure S6).

Discussion

To identify CSC specific targets, in order to design effective anti-CSCs treatment, we performed high throughput screening of breast cancer CSCs. Our microarray results confirm that CSCs derived from luminal MCF7 epithelial cell type are related to the Epithelial to Mesenchymal Transition (EMT) phenotype as it was previously suggested.[27] We identified several EMT genes (TGFB2, SNAI2 and SPARC) upregulated in CSCs isolated from MCF7 cell line. Contrarily, these genes were not up-regulated in MDA-MB-231 luminal cell line, most likely, because of the high basal expression of EMT genes in this cell line. In this context, overall data suggest that the EMT pathway

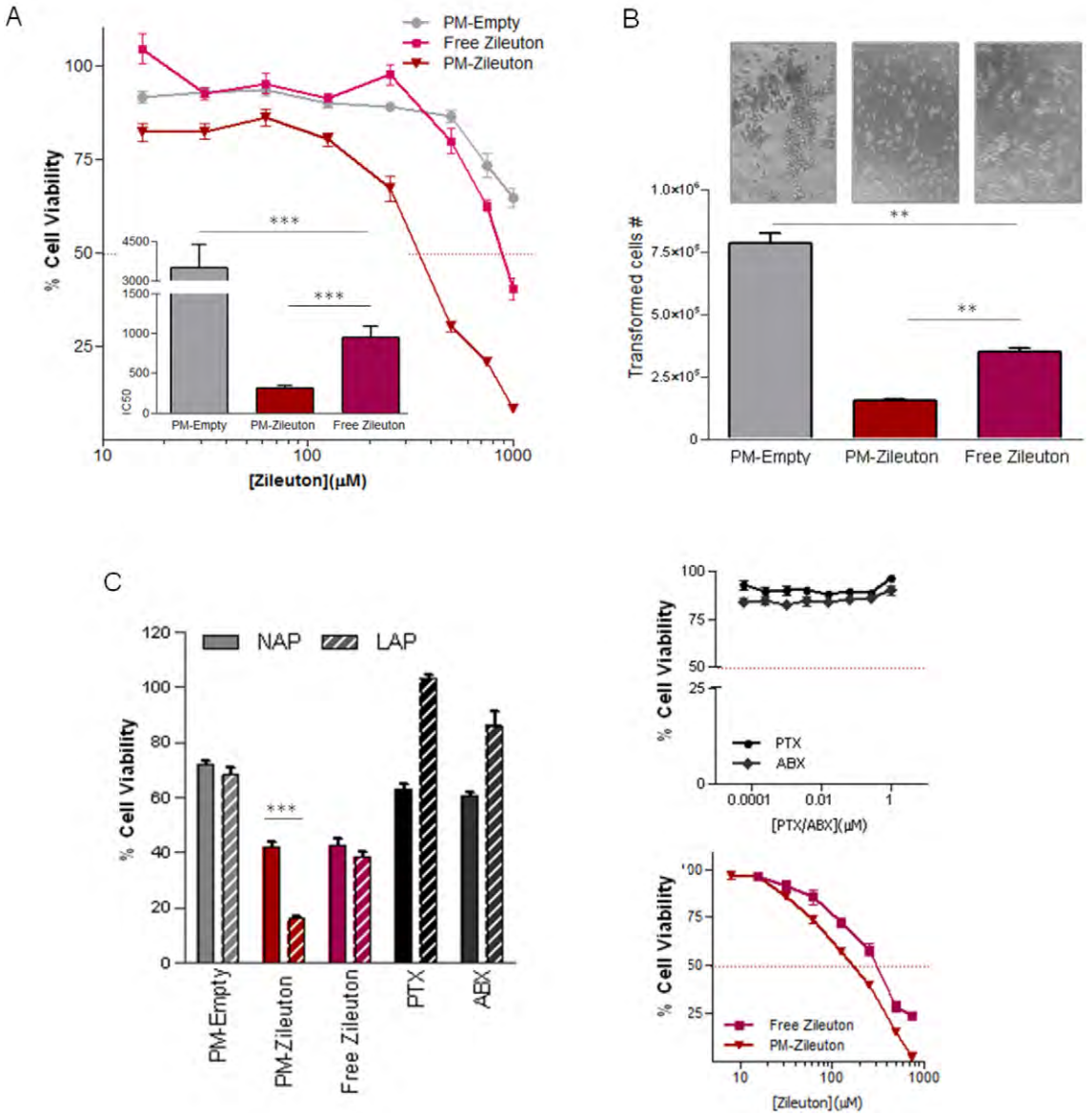

Figure 6. *In vitro* cell viability of breast cancer cell lines treated with PM-Zileuton™.(**A**) Cell viability of MDA-MB-231 cell line treated with Zileuton™ and PM-Zileuton™ and with corresponding mass of empty nanoparticles has been determined. IC_{50} corresponds to the half maximal inhibitory concentration and is indicated by a discontinuous red line. Cells without treatment represent 100% of viability.(**B**) Cell transformation assay of MDA-MB-231 treated with Zileuton™ and PM-Zileuton™ has been determined. (**C**) Cells were grown in normal condition (NAP: normal attachment plates) and as mammospheres (LAP: low attachment plates) and treated with Zileuton™ and PM-Zileuton™, PTX or ABX. IC_{50} corresponds to the half maximal inhibitory concentration and is indicated by a discontinuous red line. Cells without treatment represent 100% of viability.

may serve for effective targeting of CSCs derived from luminal breast tumors.[10,27,28] Future high throughput screening might reveal additional CSCs target candidates, because the disparity between the two analyzed cell lines can veil some less pronounced differences in gene expression when comparing CSCs *versus* non-CSCs. Nonetheless, we have found and corroborated ALOX5 overexpression in CSC subpopulations from these two highly distinctive breast cancer cell lines.

It has been reported that Alox5 deficiency resulted in a significant reduction of Leukemic Stem Cells (LSCs) in bone marrow, and thus largely prolonged survival of CML mice.[29] Importantly, there was no significant influence of Alox5 deficiency on normal hematopoietic stem cells (HSCs) or on the induction of lymphoid leukemia by BCR-ABL.[12] Besides, ALOX5 is largely known as an oncogene in solid tumors, *e.g.* prostate cancer and pancreas cancer.[30–32] On the molecular level, the inhibition of Alox5 was linked to upregulation of the tumor suppressor gene, Msr1, and consequent regulation of PI3K-AKT-GSK-3β and β-Catenin pathways (19). In this study we have further confirmed ALOX5 overexpression in a large battery of TNBC breast cancer cell lines cultured as mammospheres, in order to mimic CSCs growth. Further, clinical data confirmed its

A

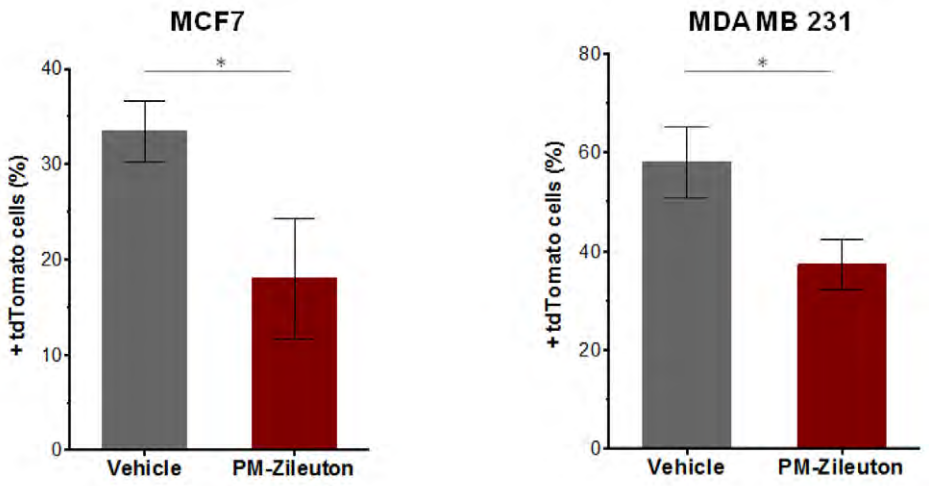

B

	CTC incidence	CSC (%)
Vehicle	6/9	35.3
PM-Zileuton	0/7	N/A

C

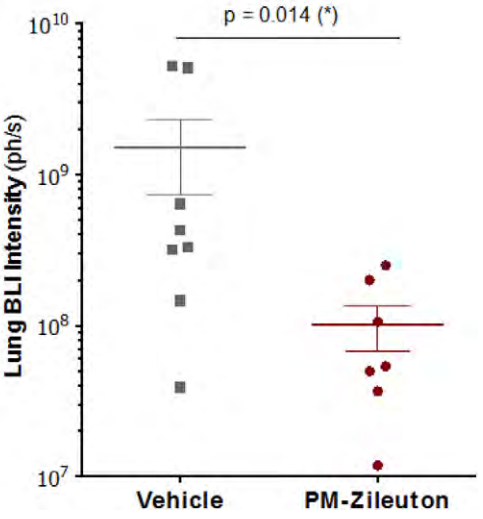

Figure 7. Effects of PM-Zileuton™ on CSC and CTC *in vivo*.Orthotopic breast cancer models were generated using tdTomato+ MDA-MB-231 cells. A posteriori, animals were then treated with i.v. administration of PM-Zileuton™ (15 mg/kg), 3 times per week during 3 weeks and blood and tumor samples were collected for the analysis of CSC content. Also lung metastasis *ex vivo* bioluminescent imaging (BLI) was performed using the IVIS Spectrum after administering 150 mg/kg of luciferin to mice. (**A**) *In vivo* effects of PM-Zileuton™ in CSC content in mice tumors; (**B**) *In vivo* effects of PM-Zileuton™ in CTC and CSC in the blood stream in tumor bearing mice; (**C**) *In vivo* effects of PM-Zileuton™ in lung metastasis.

overexpression in 86% of human breast tumors even though its overexpression was not significantly confined to any clinical feature, or any specific cancer stage. Our data suggest a potential role of Alox5 in CSC homeostasis in tumorigenesis.

Fortunately, Zileuton™, a specific inhibitor of ALOX5, is approved by the FDA for treating asthma.[14,15] Studies with Zileuton™ as anti-cancer agent are undergoing. Zileuton™ (Zyflo®) is in clinical trial (phase 1) in combination with Dasatinib (Sprycel®) (NCT02047149) and with Imatinib Mesylate (Gleevec) (NCT01130688), respectively, in patients with CML. Zileuton™ (Zyflo®) is also being investigated for lung cancer chemoprevention (currently in phase 2), with the aim to prevent lung cancer in patients with bronchial dysplasia (NCT00056004).

We have confirmed the effectiveness of its inhibition against CSCs population in various *in vitro* assays. Interestingly, Zileuton™ shows much better IC_{50} score in low attachment conditions, where just CSCs can proliferate because of their capacity to survive in non-adherent conditions, a clear feature of stemness. Of note, *ALOX5* expression is also significantly increased during these conditions. This might suggest a potential functional role of Alox5 in non-attached cells where its inhibition causes greater effect in CSC than in normal adherent culture

conditions. This further confirms the feasibility of targeting CSCs by using Zileuton™. In agreement to this, we also confirmed the anti-CSCs effects of Zileuton™ by using transformation assays in soft agar, one of the hallmarks of CSCs.

Nonetheless, Zileuton™ efficacy dose is considerably high in terms of future clinical use. Moreover, because of its highly hydrophobicity, Zileuton™ also needs to be solubilized for i.v. administration. Here, we used versatile amphiphilic polymer, Pluronic® F127 to encapsulate Zileuton™. It is an FDA approved biodegradable polymer with known characteristics and proved advantages for synthesis of drug delivery systems, and its usefulness has been demonstrated previously in various drug delivery systems.[10,11,24,25] We employed a thin-film hydration technique to synthesize polymeric micelles with Zileuton™ encapsulated in their hydrophobic inner core. Importantly, due to their stability and the possibility of lyophilization, PM-Zileuton™ are easily scalable for future Good Manufacturing Practice (GMP) production in order to facilitate posterior translation and clinical implementation.

Furthermore, we do not observe any toxicity *in vivo* when using the maximal feasible dose (MFD) (15 kg/mg). This dose was calculated based on maximal encapsulation dose and volume that can be injected per mice. The biodistribution assay performed with DiR labeled PM in tumor bearing mice shows very good accumulation of PM within the tumor. On the other hand, fluorescent signals in plasma, kidneys, lungs and muscle clearly diminish between 24 and 72 h, indicating that micelles are cleared out from these organs.

As expected, CSCs population is significantly decreased in both CSCs orthotopic models after PM-Zileuton™ treatment and importantly, in the highly metastatic MDA-MB-231cell line we observe a complete eradication of CTCs in the blood stream. Because CTCs and particularly, the fraction of CSCs within them are thought to be responsible for metastatic spread, we hypothesized an effect of PM-Zileuton™ treatment on tumor dissemination. Our data confirms that metastatic foci from MDA-MB-231 in our orthotopic *in vivo* model are significantly smaller after PM-Zileuton™ treatment suggesting a clear potential use of PM-Zileuton™ as anti-metastatic agent. This further suggests that PM-Zileuton™ could show synergistic efficacy in combination with current cytotoxic treatments, which might be highly relevant to improve current *Standard-of-Care* therapies. Of note, therapies seeking for the elimination of CSCs in order to prevent tumor growth and the appearance of metastases have an important limitation. Eliminated CSCs are constantly replaced by new cells with stemness phenotype by a process of de-differentiation (so call reversion) of non-CSC in order to ensure tumor survival and propagation after treatment. As a result, CSCs specific treatments have just limited clinical success, so far. We thus propose to evaluate the combination of PM-Zileuton™ and *Standard-of-Care* treatments (*i.e.*, Abraxane™ (Nab-PTX) nanoparticles), used in the clinical setting. This cocktail may represent an ideal option to abrogate tumor and metastatic growth, along with avoiding CSC reversion.

Appendix A. Supplementary data

Supplementary data to this article can be found online at https://doi.org/10.1016/j.nano.2019.102106.

References

1. Li R, Zhang K, Siegal GP, Wei S. Clinicopathological factors associated with survival in patients with breast cancer brain metastasis. *Hum Pathol* 2017 Jun;**64**:53-60.
2. Shen T, Gao C, Zhang K, Siegal GP, Wei S. Prognostic outcomes in advanced breast cancer: the metastasis-free interval is important. *Hum Pathol* 2017 Dec;**70**:70-6.
3. Lee G, Hall RR, Ahmed AU. Cancer stem cells: cellular plasticity, niche. *and its Clinical Relevance J Stem Cell Res Ther* 2016 Oct;**6**(10).
4. Gener P, Rafael DF, Fernandez Y, Ortega JS, Arango D, Abasolo I, et al. Cancer stem cells and personalized cancer nanomedicine. Nanomedicine (Lond) 11: 307–320.
5. Dean M, Fojo T, Bates S. Tumour stem cells and drug resistance. Nat Rev Cancer 5: 275–284.
6. Shen S, Xia JX, Wang J. Nanomedicine-mediated cancer stem cell therapy. Biomaterials 74: 1–18.
7. Vinogradov S, Wei X. Cancer stem cells and drug resistance: the potential of nanomedicine. Nanomedicine (Lond) 7: 597–615.
8. Gener P, Gouveia LP, Sabat GR, Sousa Rafael DF, Fort NB, et al. Fluorescent CSC models evidence that targeted nanomedicines improve treatment sensitivity of breast and colon cancer stem cells. *Nanomedicine* 2015 Nov;11(8):1883–92 .
9. Gener P, Rafael D, Seras-Franzoso J, Perez A, Pindado LA, Casas G, et al. Pivotal role of AKT2 during dynamic phenotypic change of breast cancer stem cells. *Cancers (Basel)* 2019 Jul 26;**11**(8), https://doi.org/10.3390/cancers11081058 (pii: E1058).
10. Rafael D, Martinez F, Andrade F, Seras-Franzoso J, Garcia-Aranda N, Gener P, et al. Efficient EFGR mediated siRNA delivery to breast cancer cells by cetuximab functionalized Pluronic® F127/Gelatin. *Chem Eng J* 2018;**340**:81-93.
11. Rafael D, Gener P, Andrade F, Seras-Franzoso J, Montero S, Fernandez Y, et al. AKT2 siRNA delivery with amphiphilic-based polymeric micelles show efficacy against cancer stem cells. *Drug Deliv* 2018 Nov;**25**(1):961-72.
12. Chen Y, Li DF, Li S, Chen Y, Hu YF, Zhang HF, et al. The Alox5 gene is a novel therapeutic target in cancer stem cells of chronic myeloid leukemia. *Cell Cycle* 2009 Nov 1;**8**(21):3488-92.
13. Rafael D, Andrade F, Montero S, Gener P, Seras-Franzoso J, Martínez F, et al. Rational design of a siRNA delivery system: ALOX5 and cancer stem cells as therapeutic targets. Prec Nanomed 2: 86–105.
14. Carter GW, Young PR FAU, Albert DH FAU, Bouska JF, Dyer RF, Bell RL et al. 5-lipoxygenase inhibitory activity of zileuton. *J Pharmacol Exp Ther* 1991 Mar;256(3):929–37 -37.
15. Poff CD, Balazy M. Drugs that target lipoxygenases and leukotrienes as emerging therapies for asthma and cancer. *Curr Drug Targets Inflamm Allergy* 2004 Mar;**3**(1):19-33.
16. Ritchie ME, Silver JF, Oshlack AF, Holmes MF, Diyagama DF, Holloway AF, et al. A comparison of background correction methods for two-colour microarrays. *Bioinformatics* 2007 Oct 15;**23**(20):2700-7.
17. Parrish RS, Spencer HJ. Effect of normalization on significance testing for oligonucleotide microarrays. *J Biopharm Stat* 2004 Aug;**14**(3):575-89.
18. Smyth GK. Linear models and empirical bayes methods for assessing differential expression in microarray experiments. *Stat Appl Genet Mol Biol* 2004;**3**(5523):5541.
19. Liang K. False discovery rate estimation for large-scale homogeneous discrete p-values. *Biometrics* 2016 Jun;**72**(2):639-48.

20. Chen Y, Sullivan C, Peng C, Shan Y, Hu Y, Li D, et al. A tumor suppressor function of the Msr1 gene in leukemia stem cells of chronic myeloid leukemia. *Blood* 2011 Jul 14;**118**(2):390-400.
21. Mendez O, Peg VA, Salvans C, Pujals M, Fernandez Y, Abasolo I, et al. Extracellular HMGA1 promotes tumor invasion and metastasis in triple-negative breast cancer. *Clin Cancer Res* 2018 Dec 15;**24**(24):6367-82.
22. Zong Y, Wu J, Shen K. Nanoparticle albumin-bound paclitaxel as neoadjuvant chemotherapy of breast cancer: a systematic review and meta-analysis. Oncotarget 2017 Mar 7;8(10):17360–17372 doi: 10 18632/oncotarget 14477 -17372.
23. Schettini F, Giuliano M, De PS, Arpino G. Nab-paclitaxel for the treatment of triple-negative breast cancer: rationale. *clinical data and future perspectives Cancer Treat Rev* 2016 Nov;**50**:129-41.
24. Andrade F, Fonte P, Costa A, Reis CC, Nunes R, Almeida A, et al. Pharmacological and toxicological assessment of innovative self-assembled polymeric micelles as powders for insulin pulmonary delivery. *Nanomedicine (Lond)* 2016 Sep;**11**(17):2305-17.
25. Andrade F, Fonte P, Oliva M, Videira M, Ferreira D, Sarmento B. Solid state formulations composed by amphiphilic polymers for delivery of proteins: characterization and stability. *Int J Pharm* 2015;**486**(1–2):195-206.
26. Andrade F. das NJ, Gener P, – Schwartz S Jr, Ferreira D, Oliva M, Sarmento B. Biological assessment of self-assembled polymeric micelles for pulmonary administration of insulin. *Nanomedicine* 2015 Oct;**11**(7):1621-31.
27. Gener P, Seras-Franzoso J, Gonzales Callego P, Andrade F, Rafael D, et al. Dynamism, sensitivity, and consequences of mesenchymal and stem-like phenotype of cancer cells. *Stem Cells International* 2018 Oct 10;**4516**:4524.
28. Rafael D, Doktorovova S, Florindo H, Gener P, Abasolo I, Schwartz Jr S, et al. EMT blockage strategies: targeting Akt dependent mechanisms for breast cancer metastatic behaviour modulation. *Curr Gene Ther* 2015;**15**(3):300-12.
29. Chen Y, Hu Y, Zhang H, Peng C, Li S. Loss of the Alox5 gene impairs leukemia stem cells and prevents chronic myeloid leukemia. Nat Genet 41: 783–792.
30. Sarveswaran S, Chakraborty D, Chitale D, Sears R, Ghosh J. Inhibition of 5-lipoxygenase selectively triggers disruption of c-Myc signaling in prostate cancer cells. *J Biol Chem* 2015 Feb 20;**290**(8):4994-5006.
31. Sarveswaran S, Thamilselvan VF, Brodie CF, Ghosh J. Inhibition of 5-lipoxygenase triggers apoptosis in prostate cancer cells via down-regulation of protein kinase C-epsilon. *Biochim Biophys Acta* 2011 Dec;**1813**(12):2108-17.
32. Zhou GX, Ding XL, Wu SB, Zhang HF, Cao W, Qu LS, et al. Inhibition of 5-lipoxygenase triggers apoptosis in pancreatic cancer cells. *Oncol Rep* 2015 Feb;**33**(2):661-8.